

Supporting Information

A Separation MOF with O/N Active Sites in Nonpolar Pore for One-step C₂H₄ Purification from C₂H₆ or C₃H₆ Mixtures

Yong-Zhi Li^a, Gang-Ding Wang^b, Rajamani Krishna^c, Qing Yin^a, Danyang Zhao^a, Jiqui Qi^a, Yanwei Sui^{a*},
and Lei Hou^{b*}

^aSchool of Materials and Physics, China University of Mining and Technology, Xuzhou 221116, P. R. China

^bKey Laboratory of Synthetic and Natural Functional Molecule of the Ministry of Education, College of Chemistry & Materials Science, Northwest University, Xi'an 710069, P. R. China.

^cVan 't Hoff Institute for Molecular Sciences, University of Amsterdam 1098 XH Amsterdam (The Netherlands)

*To whom correspondence should be addressed. E-mail: lhou2009@nwu.edu.cn (Lei Hou); wyds123456@outlook (Yanwei Sui).

Materials and general methods

All solvents and organic ligand for synthesis were purchased commercially from The Shanghai Tensus Bio-tech Co., Ltd. Elemental analyses of C, H, and N were determined with a Perkin-Elmer 2400C elemental analyzer. Thermalgravimetric analyses (TGA) were carried out in a nitrogen stream using a Netzsch TG209F3 equipment at a heating rate of 10 °C min⁻¹. Single crystal diffraction data were collected on a Bruker SMART APEX II CCD single crystal diffractometer. Gas adsorption measurements were performed with an automatic volumetric sorption apparatus (Micrometrics ASAP 2020M). Water sorption was collected by Quantachrome Vstar vapor adsorption equipment. Breakthrough experiments were performed on a Quantachrome dynaSorb BT equipments.

X-Ray Crystallography

A Bruker Smart Apex II CCD detector was used to collect the single crystal data at 216(2) K using Mo K α radiation ($\lambda = 0.71073 \text{ \AA}$). The structure was solved by direct methods and refined by full-matrix least-squares refinement based on F^2 with the Olex 2 program. The non-hydrogen atoms were refined anisotropically with the hydrogen atoms added at their geometrically ideal positions and refined isotropically. As the disordered solvent molecules in the structure cannot be located, the SQUEEZE routine of Platon program was applied in refining. The formula of complex was got by the single crystal analysis together with elemental microanalyses and TGA data. Relevant crystallographic results are listed in Table S1. Selected bond lengths and angles are provided in Table S2.

N₂ Sorption Isotherm

Before gas sorption experiments, All the as-synthesized samples were immersed in acetone for 3 days, during which the solvent was decanted and freshly replenished three times a day. All the samples were activated under vacuum at 333 K for 4 hours to obtain activated **1a**. Gas sorption measurements were then conducted using a Micrometrics ASAP 2020M gas adsorption analyzer.

Transient breakthrough simulations

Transient breakthrough simulations were carried out for the same set of operating conditions as in the experimental data sets, using the methodology described in earlier publications.¹⁻⁵ In

these simulations, intra-crystalline diffusion influences are ignored. For **1a**, there is excellent match between the experiments and simulations. From the breakthrough simulations, the productivities of 99.9% pure C₂H₄ were determined; these are expressed in the units of L per kg of **1a**.

Breakthrough Experiments

The breakthrough experiment was performed on the Quantachrome dynaSorb BT equipments at 298 K and 1 bar with an equal volume of mixed gas (gas A: gas B: Ar = 5% : 5% : 90%, Ar as the carrier gas, flow rate = 5 mL min⁻¹). The activated MOF (1 g) was filled into a packed column of ϕ 4.2×80 mm, and then the packed column was washed with Ar at a rate of 7 mL min⁻¹ at 333 K for 35 minutes to further activate the samples. Between two breakthrough experiments, the adsorbent was regenerated by Ar flow of 7 mL min⁻¹ for 35 min at 333 K to guarantee a complete removal of the adsorbed gases.

GCMC Simulation

Grand canonical Monte Carlo (GCMC) simulations were performed for the gas adsorption in the framework by the Sorption module of Material Studio (Accelrys. Materials Studio Getting Started, release 5.0). The framework was considered to be rigid, and the optimized gas and epoxide molecules were used. The partial charges for atoms of the framework were derived from QEq method and QEq neutral 1.0 parameter. One unit cell was used during the simulations. The interaction energies between the gas molecules and framework were computed through the Coulomb and Lennard-Jones 6-12 (LJ) potentials. All parameters for the atoms were modeled with the universal force field (UFF) embedded in the MS modeling package. A cutoff distance of 12.5 Å was used for LJ interactions, and the Coulombic interactions were calculated by using Ewald summation. For each run, the 5 × 10⁶ maximum loading steps, 5 × 10⁶ production steps were employed.

Fitting of experimental data on pure component isotherms

The unary isotherm data for C₂H₄, C₂H₆, and C₃H₆, measured at two different temperatures 273 K, and 298 K in **1a** were fitted with good accuracy using the dual-site Langmuir-Freundlich model, where we distinguish two distinct adsorption sites A and B:

$$q = \frac{q_{sat,A} b_A p^{v_A}}{1 + b_A p^{v_A}} + \frac{q_{sat,B} b_B p^{v_B}}{1 + b_B p^{v_B}} \quad (S1)$$

In eq (S1), the Langmuir-Freundlich parameters b_A, b_B are both temperature dependent

$$b_A = b_{A0} \exp\left(\frac{E_A}{RT}\right); \quad b_B = b_{B0} \exp\left(\frac{E_B}{RT}\right) \quad (S2)$$

In eq (S2), E_A, E_B are the energy parameters associated with sites A, and B, respectively.

The fit parameters are provided in Table S3,

Isosteric heat of adsorption

The isosteric heat of adsorption, Q_{st} , is defined as

$$Q_{st} = -RT^2 \left(\frac{\partial \ln p}{\partial T} \right)_q \quad (S3)$$

where the derivative in the right member of eq (S3) is determined at constant adsorbate loading, q . The derivative was determined by analytic differentiation of the combination of eq (S1), eq (S2), and eq (S3).

Gas Selectivity Prediction via IAST

The experimental isotherm data for pure C_2H_4 , C_2H_6 and C_3H_6 were fitted using a dual Langmuir-Freundlich (L-F) model:

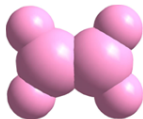
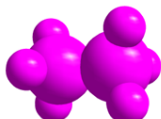
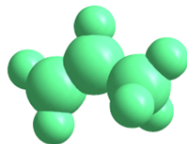
$$q = \frac{a_1 * b_1 * P^{c_1}}{1 + b_1 * P^{c_1}} + \frac{a_2 * b_2 * P^{c_2}}{1 + b_2 * P^{c_2}}$$

Where q and p are adsorbed amounts and the pressure of component i , respectively.

The adsorption selectivities for binary mixtures, defined by

$$S_{i/j} = \frac{x_i^* y_j}{x_j^* y_i}$$

Were respectively calculated using the Ideal Adsorption Solution Theory (IAST). Where x_i is the mole fraction of component i in the adsorbed phase and y_i is the mole fraction of component i in the bulk.

Molecular structure						
Molecular formula	Molecular Dimension (Å)			Kinetic diameter (Å)	Polarizability × 10 ⁻²⁵ (cm ³)	Boiling point(K)
	X	Y	Z			
C ₂ H ₄	3.28	4.18	4.84	4.16	42.5	169.4
C ₂ H ₆	3.81	4.08	4.82	4.44	44.3-44.7	184.6
C ₃ H ₈	4.20	5.30	6.40	4.68	62.6	225.5

Scheme S1. Structures and physical properties of C₂H₄, C₂H₆ and C₃H₈.

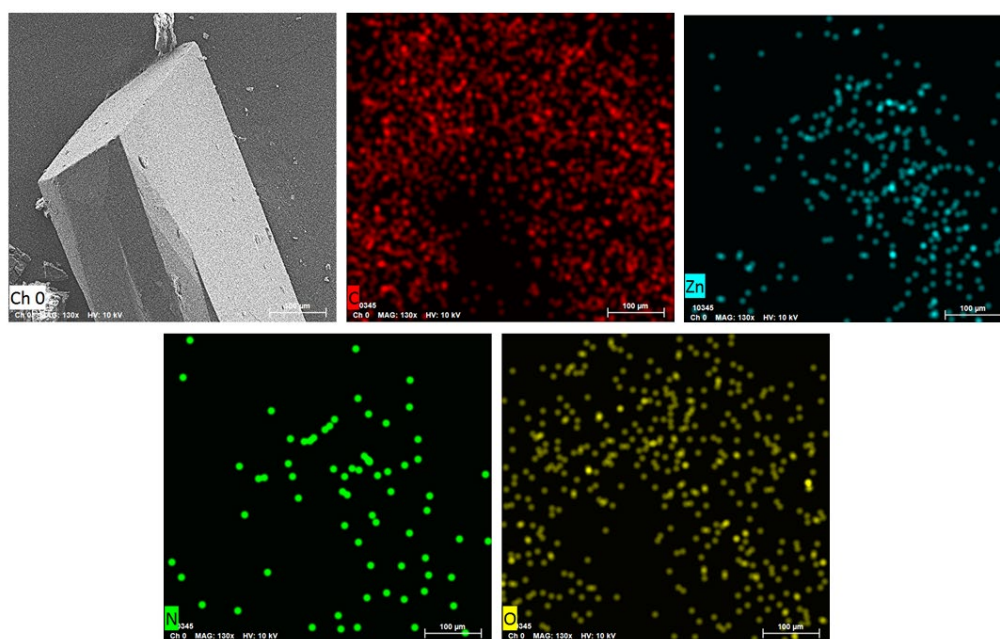


Figure S1. SEM images of as-synthesized MOF, and elemental mapping from SEM-EDX showing uniform distribution of elements (mixed elements, C, Zn, N, O) in the selected area of crystal.

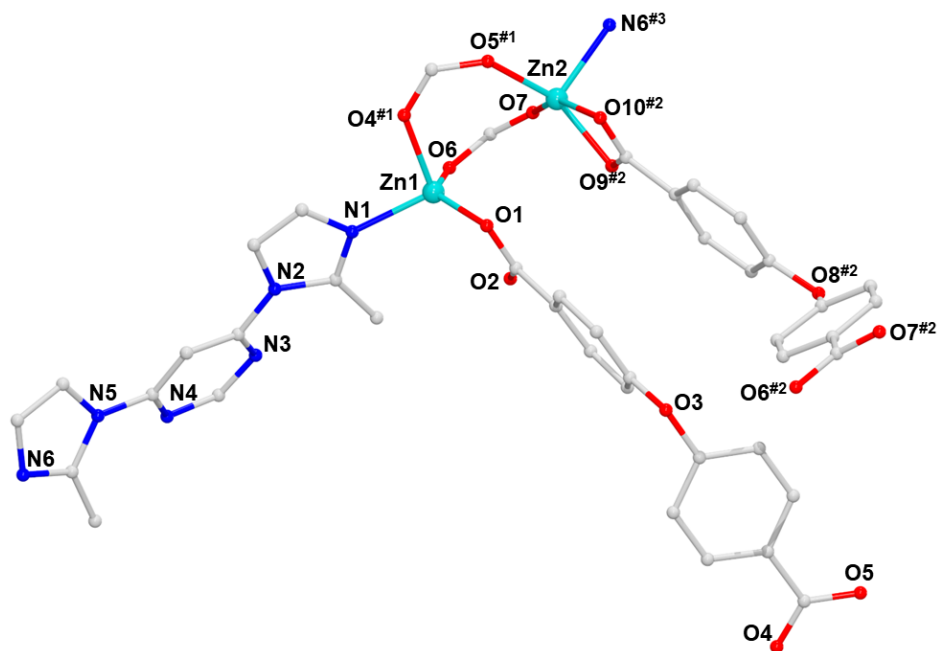


Figure S2. Coordination environment of Zn(II) ions.

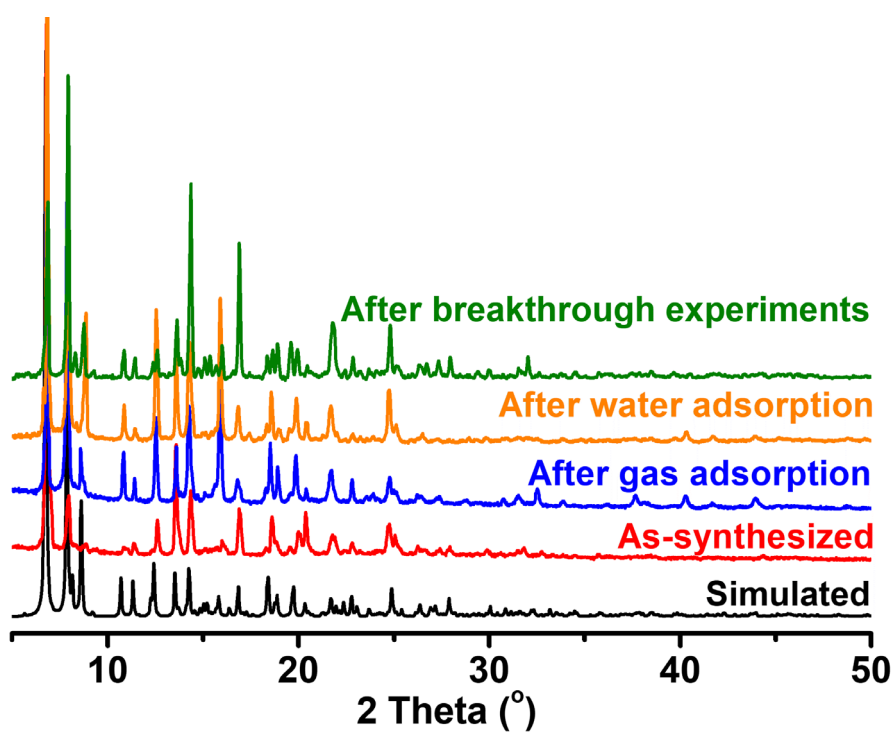


Figure S3. PXRD patterns of 1.

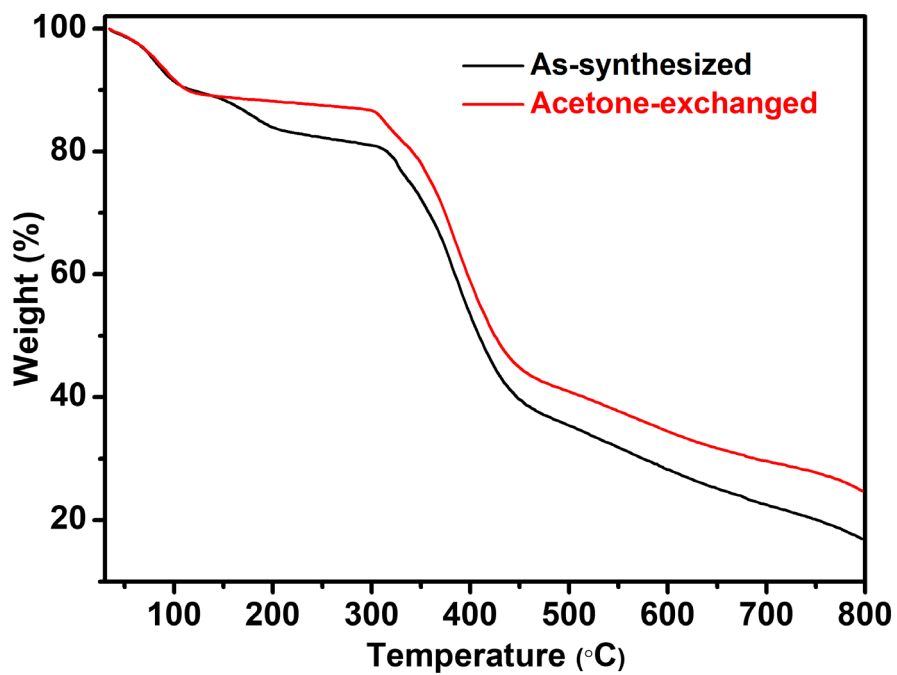


Figure S4. TGA curves of as-synthesized and acetone-exchanged samples of **1**.

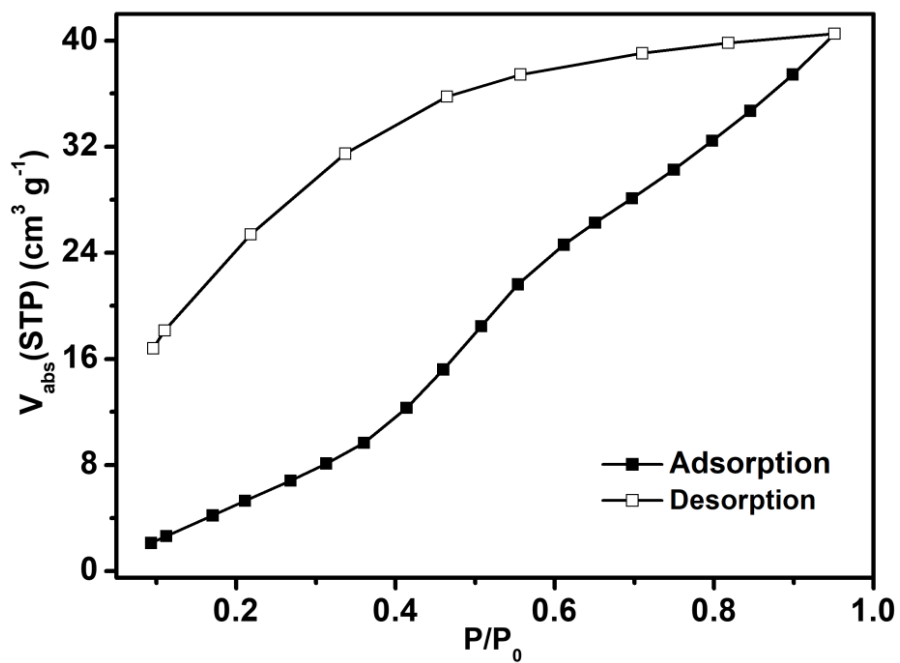


Figure S5. Water vapor adsorption and desorption isotherm of **1a** at 298 K.

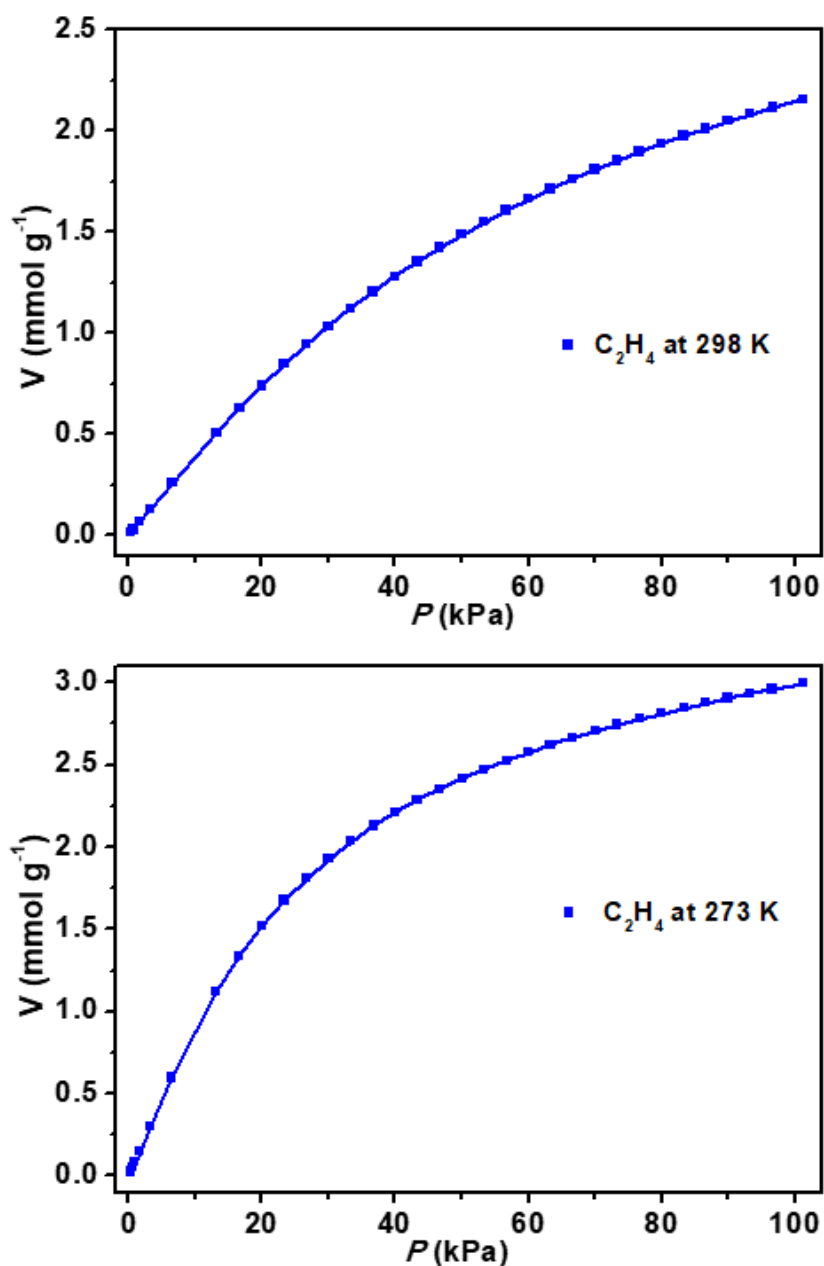


Figure S6. C₂H₄ adsorption isotherms of **1a** with fitted by dual L-F model at 298 K and 273 K, 298 K: $a_1 = 3.43606$, $b_1 = 0.00921$, $c_1 = 1.12333$, $a_2 = 0.01901$, $b_2 = 0.6084$, $c_2 = 1.18178$, $\text{Chi}^2 = 3.4532\text{E-}7$, $R^2 = 1$; 273 K: $a_1 = 3.52331$, $b_1 = 0.02478$, $c_1 = 1.14267$, $a_2 = 0.17732$, $b_2 = 2.1274\text{E-}9$, $c_2 = 4.25404$, $\text{Chi}^2 = 0.00002$, $R^2 = 0.99999$.

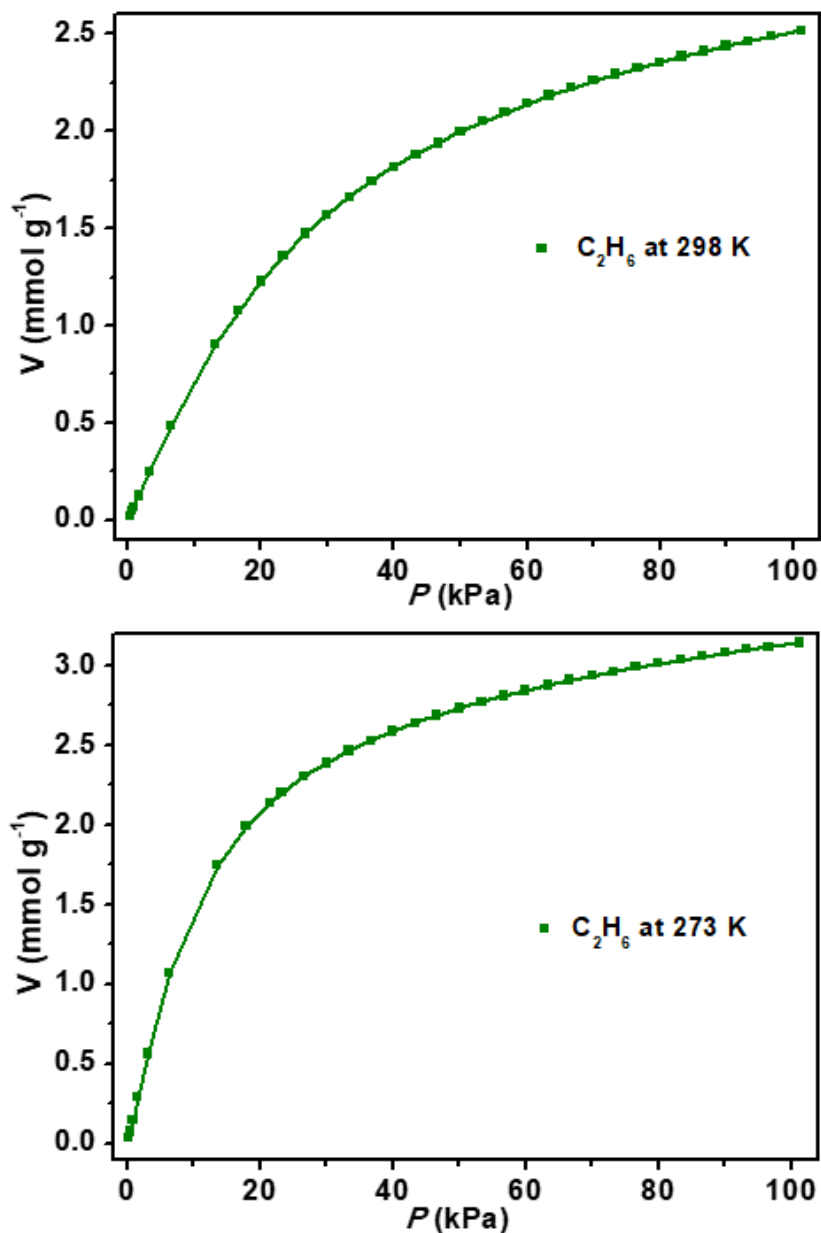


Figure S7. C₂H₆ adsorption isotherms of **1a** with fitted by dual L-F model at 298 K and 273 K, 298 K: $a_1 = 3.06171$, $b_1 = 0.02323$, $c_1 = 1.12105$, $a_2 = 0.09758$, $b_2 = 2.3658E-9$, $c_2 = 4.34811$, $\text{Chi}^2 = 8.1286E-6$, $R^2 = 0.99999$; 273 K: $a_1 = 2.97636$, $b_1 = 0.05995$, $c_1 = 1.20031$, $a_2 = 0.8132$, $b_2 = 0.00025$, $c_2 = 1.73607$, $\text{Chi}^2 = 0.00003$, $R^2 = 0.99998$.

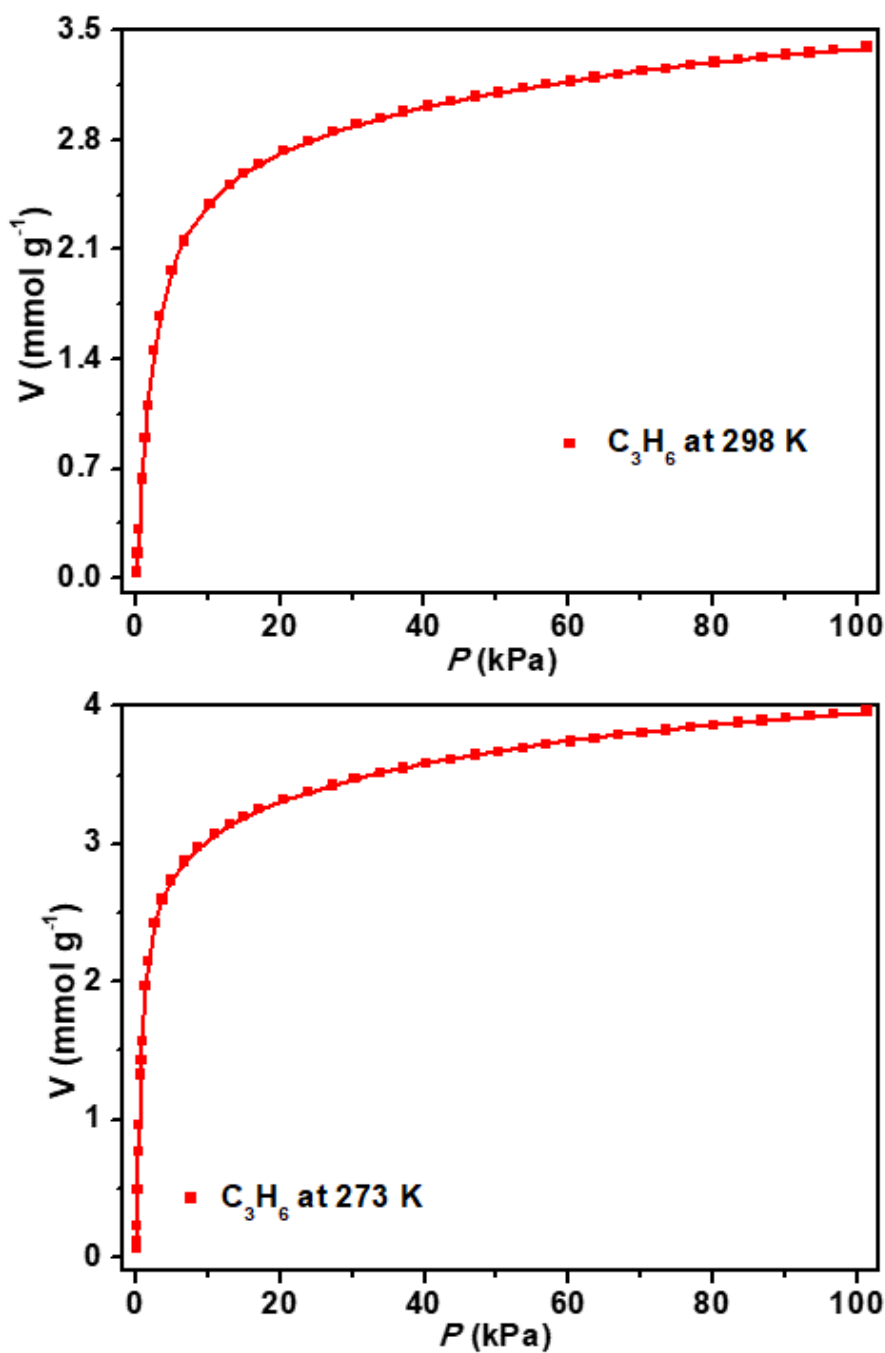


Figure S8. C_3H_6 adsorption isotherms of **1a** with fitted by dual L-F model at 298 K and 273 K, 298 K: $a_1 = 2.60175$, $b_1 = 0.38696$, $c_1 = 1.20055$, $a_2 = 1.34085$, $b_2 = 0.01105$, $c_2 = 1.06743$, $\chi^2 = 0.00002$, $R^2 = 0.99998$; 273 K: $a_1 = 2.6841$, $b_1 = 0.10486$, $c_1 = 0.59355$, $a_2 = 2.29332$, $b_2 = 1.83345$, $c_2 = 1.41842$, $\chi^2 = 0.00004$, $R^2 = 0.99997$.

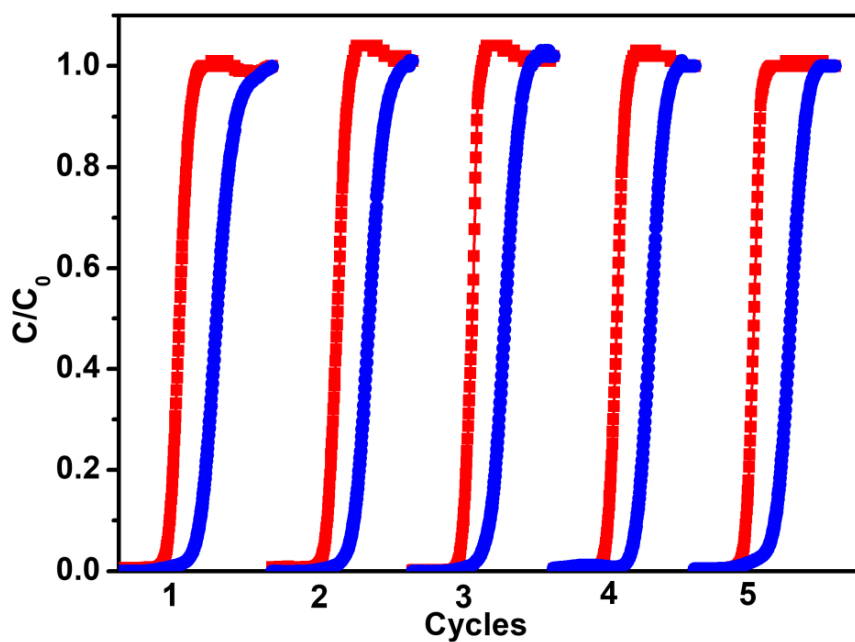


Figure S9. Cycling tests for equimolar C_2H_6/C_2H_4 mixture at 298 K.

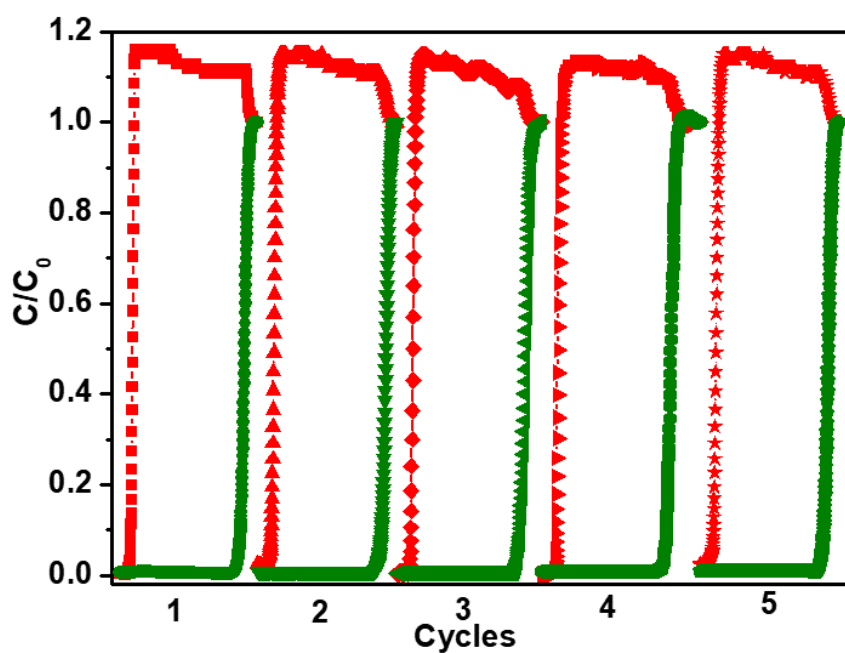


Figure S10. Cycling tests for equimolar C_3H_6/C_2H_4 mixture at 298 K.

Table S1. Crystal Data and Structure Refinements for **1**.

Chemical formula	C ₄₀ H ₂₈ Zn ₂ N ₆ O ₁₀
Formula weight	883.42
<i>T</i> (K)	216(2)
Crystal system, Space group	Triclinic, <i>P</i> -1
<i>a</i> (Å)	13.0194(4)
<i>b</i> (Å)	14.4119(4)
<i>c</i> (Å)	16.3911(4)
α (°)	87.5590(10)
β (°)	72.9610(10)
γ (°)	65.3030(10)
<i>V</i> (Å ³)	2660.26(13)
<i>Z</i>	2
<i>D</i> _{calcd.} [g·cm ⁻³]	1.103
μ (mm ⁻¹)	0.950
Reflns collected/unique/ <i>R</i> _{int}	42527/9700/0.0369
Goof	1.051
<i>R</i> ₁ ^a , <i>wR</i> ₂ ^b [<i>I</i> > 2 σ]	<i>R</i> ₁ = 0.0367, <i>wR</i> ₂ = 0.1055
<i>R</i> ₁ ^a , <i>wR</i> ₂ ^b (all data)	<i>R</i> ₁ = 0.0482, <i>wR</i> ₂ = 0.1118

$$^aR_1 = \Sigma(|F_o| - |F_c|) / \Sigma|F_o|. \quad ^bR_2 = [\Sigma w(F_o^2 - F_c^2)^2 / \Sigma w(F_o^2)]^{1/2}.$$

Table S2. Selected bond lengths [Å] and angles [°] for **1**.

Zn(1)-O(5)	1.9501(18)	O(5)-Zn(1)-N(6)#3	99.62(8)
Zn(1)-O(7)#1	1.9801(19)	O(7)#1-Zn(1)-N(6)#3	98.29(9)
Zn(1)-O(10)#2	1.9576(18)	O(10)#2-Zn(1)-O(7)#1	103.77(8)
Zn(1)-N(6)#3	2.033(2)	O(10)#2-Zn(1)-N(6)#3	106.41(8)
Zn(2)-O(1)	1.9384(19)	O(1)-Zn(2)-O(4)#4	104.17(8)
Zn(2)-O(4)#4	1.9952(19)	O(1)-Zn(2)-O(6)	130.37(9)
Zn(2)-O(6)	1.9404(19)	O(1)-Zn(2)-N(1)	115.05(9)
Zn(2)-N(1)	2.007(2)	O(4)#4-Zn(2)-N(1)	96.21(8)
O(5)-Zn(1)-O(7)#1	106.20(8)	O(6)-Zn(2)-O(4)#4	101.75(9)
O(5)-Zn(1)-O(10)#2	136.55(8)	O(6)-Zn(2)-N(1)	103.19(9)

Symmetry codes: #1 *x*, *y*+1, *z*; #2 *x*-1, *y*+2, *z*; #3 *x*, *y*+1, *z*; #4 *x*, *y*-1, *z*; #5 *x*+1, *y*-2, *z*; #6 *x*, *y*-1, *z*+1.

Table S3. Dual-site Langmuir-Freundlich fits for C₂H₄, C₂H₆, and C₃H₆, in **1a**.

	Site A				Site B			
	$\frac{q_{A,sat}}{\text{mol kg}^{-1}}$	$\frac{b_{A,0}}{\text{Pa}^{-\nu_A}}$	$\frac{E_A}{\text{kJ mol}^{-1}}$	ν_A	$\frac{q_{B,sat}}{\text{mol kg}^{-1}}$	$\frac{b_{B,0}}{\text{Pa}^{-\nu_B}}$	$\frac{E_B}{\text{kJ mol}^{-1}}$	ν_B
C ₂ H ₄	2.2	1.951E-09	24	0.83	2.1	7.38E-12	30	1.25
C ₂ H ₆	2.2	7.684E-09	23.3	0.75	2	6.65E-12	31.5	1.3
C ₃ H ₆	2.1	2.855E-13	44.5	1.44	2.6	5.45E-08	24	0.61

References

- S1 R. Krishna, The Maxwell-Stefan Description of Mixture Diffusion in Nanoporous Crystalline Materials, *Microporous Mesoporous Mater.* **2014**, 185, 30-50.
- S2 R. Krishna, Methodologies for Evaluation of Metal-Organic Frameworks in Separation Applications, *RSC Adv.* **2015**, 5, 52269-52295.
- S3 R. Krishna, Screening Metal-Organic Frameworks for Mixture Separations in Fixed-Bed Adsorbers using a Combined Selectivity/Capacity Metric, *RSC Adv.* **2017**, 7, 35724-35737.
- S4 R. Krishna, Methodologies for Screening and Selection of Crystalline Microporous Materials in Mixture Separations, *Sep. Purif. Technol.* **2018**, 194, 281-300.
- S5 R. Krishna, Metrics for Evaluation and Screening of Metal-Organic Frameworks for Applications in Mixture Separations, *ACS Omega* **2020**, 5, 16987-17004.